

LOW DARK MATTER CONTENT OF THE NEARBY EARLY-TYPE GALAXY NGC 821

S. Samurović, A. Vudragović, M. Jovanović and M. M. Ćirković

Astronomical Observatory, Volgina 7, 11160 Belgrade 74, Serbia

E-mail: *srdjan@aob.rs*

(Received: March 26, 2014; Accepted: May 27, 2014)

SUMMARY: In this paper we analyze the kinematics and dynamics of the nearby early-type galaxy NGC 821 based on its globular clusters (GCs) and planetary nebulae (PNe). We use PNe and GCs to extract the kinematics of NGC 821 which is then used for the dynamical modelling based on the Jeans equation. We apply the Jeans equation using the Newtonian mass-follows-light approach assuming constant mass-to-light ratio and find that using such an approach we can successfully fit the kinematic data. The inferred constant mass-to-light ratio, $4.2 < M/L_B < 12.4$ present throughout the whole galaxy, implies the lack of significant amount of dark matter. We also used three different MOND approaches and found that we can fit the kinematic data without the need for additional, dark, component.

Key words. dark matter – galaxies: elliptical and lenticular – galaxies: kinematics and dynamics – galaxies: structure

1. INTRODUCTION

The problem of mere existence of dark matter in early-type galaxies remains one of the biggest unsolved questions in the contemporary extragalactic astronomy and cosmology, and the problems one faces in the study of dark matter in early-type galaxies are listed in e.g. Samurović (2007, Chap. 1). Some recent research suggests that some nearby galaxies such as NGC 5128 appear to lack dark matter, or at least dark matter is not dynamically important out to approximately 6 effective radii (R_e) (see Samurović 2010). On the other hand, Samurović (2012) recently analyzed the massive early-type galaxy NGC 4472 and found that beyond $\sim 2R_e$ dark matter or modifications of Newtonian dynamics are necessary to successfully fit the observed velocity dispersion. Also recently, Deason et al. (2012), studied a sample of 15 elliptical galax-

ies out to $\sim 5R_e$ using tracers such as planetary nebulae (PNe) and globular clusters (GCs), and found that, in general, the galaxies that they studied are dominated by dark matter in their outer parts (beyond $\sim 2R_e$). Because of the fact that the sample of the studied early-type galaxies is still small, it is important to study, whenever possible, an object for which the observational data out to several effective radii is available.

Since it is a well-established fact that spiral galaxies are found in massive dark haloes one can expect that all early-type galaxies also contain a significant amount of dark matter. The analyses of early-types in the available literature usually rely on Newtonian dynamics to reach conclusions. However, the MOND (MODified Newtonian Dynamics) (Milgrom 1983) theory, already well tested on spirals, proved to be capable of successfully fitting early-type galaxies in some cases, but not always. The basic assumption of MOND is the fact that the acceleration due

to gravitational force which does not depend simply upon mass m as in the Newtonian approach, but has a more complex form, $m/\mu(a/a_0)$, where a_0 is the universal constant, $a_0 = 1.35_{-0.42}^{+0.28} \times 10^{-8} \text{ cm s}^{-2}$ (Famaey et al. 2007). In the MOND theory the interpolating function $\mu(x)$ assumes several forms (see Section 3.2 regarding the details on three interpolating functions used in this paper): for $a \gg a_0$, one has the Newtonian acceleration and for $a \ll a_0$ the interpolation function becomes $\mu = a/a_0$. The results regarding the application of the MOND methodology to the study of dynamics of early-type galaxies are mixed: whereas in some cases (for example, NGC 3379, see Tiret et al. (2007) and the aforementioned NGC 5128) MOND correctly describes their dynamics without the need for dark matter, in some other cases (such as NGC 1399, see Richtler et al. 2008) one needs additional dark component even if using the MOND approach.

Although the galaxy NGC 821 studied in the present paper has been a subject of several studies so far (see e.g. Deason et al. 2012 for details), we find it important to analyze it again, this time using two different sets of tracers (PNe and GCs) and two different methodologies (Newtonian and MOND) to reach the conclusions regarding the content of dark matter in it.

The plan of the paper is as follows: in Section 2 we present the details on the early-type galaxy NGC 821 and the samples of PNe and GCs that we use in this paper and we also present the kinematics of NGC 821 based on those tracers. In Section 3 we describe the theoretical aspects of the analysis of the dynamics, and in Section 4 we use the Jeans equation in both Newtonian and the MOND approach to determine the best-fit parameters for both populations of tracers. Finally, in Section 5 we present the conclusions.

2. OBSERVATIONAL DATA: THE SAMPLES

NGC 821 is classified as an isolated E6 galaxy (de Vaucouleurs 1991) and its absolute B -band magnitude is equal to -20.82 . The distance we use in this paper is $D = 23.4 \pm 1.9 \text{ Mpc}$ (from Tonry et al. 2001, with corrections from Mei et al. 2007), which means that 1 arcsec in this galaxy corresponds to 113.50 pc and 1 arcmin corresponds to 6.81 kpc. The effective radius is $R_e = 51 \text{ arcsec}$.

In this work, we use two different samples of tracers belonging to NGC 821: the planetary nebulae (PNe) taken from Teodorescu et al. (2010, hereafter T10) and globular clusters (GCs) taken from Pota et al. (2013, hereafter P13). We use these tracers in order to extract kinematics which we then model using the Jeans equation, as described below.

We express the galactocentric distances of the tracers in both cases as an equivalent radius:

$$R = \sqrt{qX^2 + \frac{Y^2}{q}}, \quad (1)$$

where q is the axis ratio (ratio of the minor and major axis) of NGC 821, and X and Y are Cartesian coordinates of a given object in the rest frame of the galaxy; the center of the galaxy coincides with the origin of the coordinate system, and X (Y) is aligned with the photometric major (minor) axis. The value of the q parameter for NGC 821 is taken from P13 and is equal to: $q = 0.62$.

In Fig. 1 we present the radial distribution of the tracers in NGC 821: in the upper panel the case of PNe is given, and in the lower panel the profile based on GCs is presented. Also indicated in Fig. 1 are the values of the γ parameter coming from the linear fit of the form $N \propto R^{-\gamma}$: these values will be used below in solving the Jeans equation.

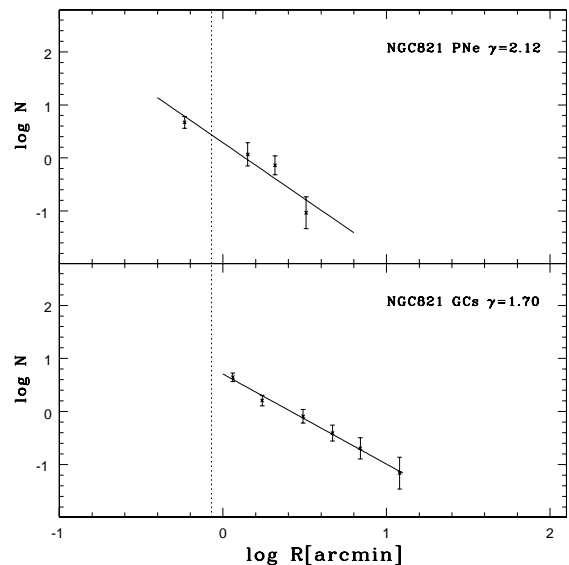


Fig. 1. Radial distribution of PNe (upper panel) and GCs (lower panel) of the early-type galaxy NGC 821. A power law is fitted with the solid lines to the radial surface density in both cases: $N \propto R^{-\gamma}$.

The kinematics of PNe (GCs) of NGC 821 is given in Fig. 2 left (right): from top to bottom are plotted: velocities of the PNe (GCs) in the sample, their velocity dispersions, and s_3 and s_4 parameters which describe symmetric and asymmetric departures from the Gaussian, respectively. The departures from the Gaussian are calculated using the standard formulas which also include the errors:

$$s_3 = \frac{1}{N} \sum_{i=1}^N \left(\frac{v_i - v_{\text{sys}}}{\sigma} \right)^3 \pm \sqrt{\frac{6}{N}} \quad (2)$$

and

$$s_4 = \left[\frac{1}{N} \sum_{i=1}^N \left(\frac{v_i - v_{\text{sys}}}{\sigma} \right)^4 \right] - 3 \pm \sqrt{\frac{24}{N}}, \quad (3)$$

where N is the number of objects per bin, v_i is the velocity of a given object, v_{sys} is the systemic velocity and σ is the velocity dispersion.

2.1. The sample of PNe of NGC 821

We use the sample of PNe from T10 obtained using a slitless spectroscopy with the 8.2 m Subaru telescope and its FOCAS Cassegrain spectrograph. In total, we have 144 PNe taken from their Table 2. We excluded the object no. 104 from the T10 sample with anomalously low heliocentric velocity of 1171 km s^{-1} since this velocity is probably wrong because of the misinterpretation of the object as 5007 \AA emitter, as explained in Notes of Table 2 from T10; the inclusion of this object in our sample would result in the low s_3 value ($s_3 \approx -2$) and extremely high value of the s_4 parameter ($s_4 \approx 6$).

From Fig. 2 (left) and Table 1 one can see that the velocity dispersion of NGC 821 has a declining trend, and at $\sim 3 \text{ arcmin}$ ($\sim 3.7R_e$) the velocity dispersion is approximately 100 km s^{-1} . The departures from the Gaussian, given with the s_3 and s_4 parameters are small and consistent with zero.

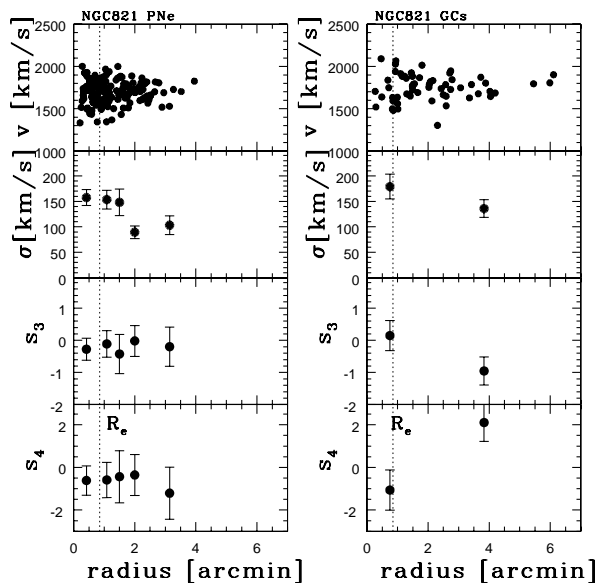


Fig. 2. Kinematics of NGC 821 based on PNe (left panel) and GCs (right). From top to bottom: radial velocity in km s^{-1} ; velocity dispersion in km s^{-1} calculated in a given bin and the s_3 and s_4 parameters, which describe symmetric and asymmetric departures from the Gaussian, respectively. The vertical dotted line in both plots denotes one effective radius. See text for details.

2.2. The sample of GCs of NGC 821

Another sample used in this paper is that coming from P13, i.e. SLUGGS (SAGES Legacy Unifying Globulars and Galaxies Survey) database¹, and is based on the GCs. This survey combines Subaru/Supreme-Cam wide-field imaging with spectra obtained using the Keck/DEep Imaging Multi Object Spectrograph (DEIMOS), and the sample of galaxies uses high velocity resolution data and includes galaxies with a wide range of luminosities, morphological types (within the early-type class) and from different environments (from field galaxies to members of groups and clusters). Our sample of tracers found in NGC 821 consists of 58 objects (blue and red GCs) in total. We note that we did not split our sample into blue and red populations in order to have larger number of objects per bin and yet we have the values of the velocity dispersion (and the departures from the Gaussian) in just two separate bins.

From Fig. 2 (right) and Table 2 one can see that the velocity dispersion of NGC 821 again shows a declining trend, and at the outer point, at $\sim 4 \text{ arcmin}$ ($\sim 4.5R_e$), the velocity dispersion is higher with respect to the previously found value in the case of PNe, and is equal to 136 km s^{-1} . The departures from the Gaussian, given with the s_3 and s_4 parameters are small. Again, we note that the number of tracers is rather low to establish the anisotropies with certainty. We, however, anticipate taking into account the radial anisotropies in our Jeans modelling below.

We note that the object responsible for a non-zero value of both s_3 and s_4 parameters is a blue GC (no. 51 in the catalog of P13) with the radial velocity of 1303 km s^{-1} . We could not exclude this object, because it is a confirmed blue GC, with color $g - i = 0.94$.

3. THE JEANS MODELLING OF NGC 821

In this Section we briefly present the approach based on the Jeans equation that we adopted in the dynamical modelling of NGC 821.

We solve the Jeans equation (e.g. Binney and Tremaine 2008) in a spherical approximation for both Newtonian and MOND approaches:

$$\frac{d\sigma_r^2}{dr} + \sigma_r^2 \frac{(2\beta_* + \alpha)}{r} = a_{N;M} + \frac{v_{\text{rot}}^2}{r}. \quad (4)$$

Here $a_{N;M}$ is an acceleration term which is different for each approach: in the Newtonian ('N') approach it is equal to $a_N = -\frac{GM(r)}{r^2}$ and for MOND ('M') models $a_M \mu(a_M/a_0) = a_N$ (see below for expressions of function μ). σ_r is the radial velocity dispersion, $\alpha = d \ln \rho / d \ln r$ is the slope of each tracer density ρ . The exponents of the power fits of the surface density

¹<http://sluggs.swin.edu.au>

for NGC 821 are indicated in Fig. 1: for example, the radial distribution for PNe was fitted with the exponent equal to -2.12 (see Fig. 1, upper panel), which means that α used in the Jeans equation is $\alpha = -3.12$. We determined negligible values of the rotational components, fully consistent with zero, for both families of tracers and thus the rotation speed v_{rot} for NGC 821 is taken zero in both cases.

The non-spherical nature of the stellar velocity dispersion is expressed using the equation:

$$\beta_* = 1 - \frac{\overline{v_\theta^2}}{\sigma_r^2}, \quad (5)$$

where $\overline{v_\theta^2} = \overline{v_\theta^2} + \sigma_\theta^2$ and $0 < \beta_* < 1$ means that the orbits are predominantly radial (equivalent to $s_4 > 0$), whereas for $-\infty \leq \beta_* < 0$ the orbits are mostly tangential (equivalent to $s_4 < 0$) (Gerhard 1993).

The projected line-of-sight velocity dispersion for all the models for the galaxies in the sample is given as (Binney and Mamon 1982):

$$\sigma_p^2(R) = \frac{\int_R^{r_t} \sigma_r^2(r) [1 - (R/r)^2 \beta_*] \rho(r) (r^2 - R^2)^{-1/2} r dr}{\int_R^{r_t} \rho(r) (r^2 - R^2)^{-1/2} r dr}, \quad (6)$$

where the truncation radius, r_t , extends beyond the observed kinematical point of the highest galactocentric radius.

Below, we study two cases of anisotropies:

a) The lack of anisotropy (the isotropic case), as the most general case ($\beta = 0$), and:

b) The theoretically based case, for which:

$$\beta(r) = \beta_0 \frac{r}{(r + r_a)}, \quad (7)$$

where $\beta_0 \simeq 0.5$ and $r_a \simeq 1.4R_e$; this estimate (obviously radially dominated, $\beta > 0$, which is important for our case for which we have an indication of radial anisotropies in the outer parts of NGC 821) comes from theoretical expectations from merging collisionless systems; we denote the values of the β parameter thus calculated as β_{th} in the text below.

3.1. Newtonian models

Within the framework of Newtonian models, we use a constant mass-to-light ratio model and consider the stellar mass being distributed in the form of the standard Hernquist (1990) profile:

$$\rho_H(r) = \frac{M_T a}{2\pi} \frac{1}{r (r + a)^3}, \quad (8)$$

that has two parameters: the total mass M_T and scale length, a , where $R_e = 1.8153a$.

We will simply vary the mass-to-light ratio to establish the best value to describe the observed velocity dispersion for both populations of tracers (PNe and GCs).

3.2. MOND models

We tested several MOND models using the Jeans equation in the spherical approximation.

The Newtonian acceleration is given as $a_N = a\mu(a/a_0)$, where a is the MOND acceleration, a_0 is the universal constant given in the Introduction and $\mu(x)$ is the MOND interpolating function which is different for each MOND model. We tested three MOND models (listed below) in order to infer whether additional dark matter component is needed and whether MOND is sufficient to correctly describe the dynamics of NGC 821.

A simple MOND formula (Famaey and Binney 2005) is given by (the expression for x is given in the Introduction and is valid in all MOND cases):

$$\mu(x) = \frac{x}{1+x}. \quad (9)$$

A standard MOND formula (Sanders and McGaugh 2002) is given by:

$$\mu(x) = \frac{x}{\sqrt{1+x^2}}. \quad (10)$$

The toy MOND model (Bekenstein 2004) is described with:

$$\mu(x) = \frac{-1 + \sqrt{1+4x}}{1 + \sqrt{1+4x}}. \quad (11)$$

The expressions for the circular velocities for the three functions are given in Samurović and Čirković (2008).

Again, we vary the mass-to-light ratio to establish which value best describes the observed velocity dispersions and the plots obtained using the best-fitting values are presented below.

4. RESULTS

Here we present the result of the Jeans modelling of the early-type galaxy NGC 821 for both Newtonian and MOND approaches and for both populations of tracers, PNe and GCs.

Before we obtain our estimates of the best-fitting values of mass-to-light ratio of NGC 821, we calculate the estimate of this quantity valid for the stellar component *only*. To this end, we use the HyperLeda database from which we take the color ($B - V = 1$), and the results of stellar population synthesis (SPS) models of Bell and De Jong (2001) to find that the *stellar* mass-to-light ratio in the B -band for NGC 821 is equal to (for metallicity $Z = 0.02$ and for the Salpeter initial mass function (IMF)):

i) $M/L_B = 9.6$ (PEGASE model) and

ii) $M/L_B = 8.7$ (Bruzual and Charlot model).

The galaxy NGC 821 was investigated in the sample of galaxies in the work of Conroy and van Dokkum (2012), who presented their new population synthesis model. Below, the two values of the

estimated mass-to-light ratio of NGC 821 in the B -band, again for metallicity $Z = 0.02$, for two various IMF are given:²

a) $M/L_B = 4.33$ (for a model that allows for IMF variation) and

b) $M/L_B = 3.64$ (for a fixed Kroupa (2001) Milky Way IMF).

The significantly higher values of the best-fitting values of the mass-to-light ratio obtained using the Jeans equation would suggest the existence of dark matter. One can see that the estimates based on the paper by Conroy and van Dokkum (2012) are approximately half the estimates coming from the models of Bell and De Jong (2001) meaning that these lower values of the mass-to-light ratio of the stellar population suggest more dark matter in NGC 821. Thus, one can conclude that dark matter is needed whenever a discrepancy between the SPS and Jeans models is encountered.

As given above, for both approaches (and for both populations of tracers) we will use two assumptions on the anisotropy: isotropic case ($\beta = 0$) and radially anisotropic case based on the theoretical expectations ($\beta_{\text{th}} > 0$, see Eq. (7)).

4.1. Newtonian models of NGC 821

The fits of NGC 821 obtained using the Jeans equation based on the Newtonian mass-follows-light approach are presented in Figs. 3 and 4 in the upper panel for PNe and GCs, respectively. The galaxy can be fitted with a constant mass-to-light ratio out to $\sim 4.5R_e$: the interval of the values that provide a successful fit to the two observational points is $4.2 < M/L_B < 7.0$ (for PNe) and $7.8 < M/L_B < 12.4$ (for GCs), or, more precisely:

1) The best-fitting values based on PNe are: $M/L_B = 5.0 \pm 0.8$ for the isotropic case and $M/L_B = 6.0 \pm 1.0$ for the anisotropic case, and:

2) The best-fitting values based on GCs are: $M/L_B = 9.4 \pm 1.6$ for the isotropic case and $M/L_B = 11.8 \pm 0.6$ for the anisotropic case.

The best-fitting values are presented in Figs. 3 and 4 in the upper panel with thick (thin) solid lines for isotropic (radially anisotropic) cases.

One can see from these results that the obtained values of the mass-to-light ratio using two different populations show a certain discrepancy and the estimates based on GCs are somewhat higher than those based on PNe. Note, however, that the number of GCs is much lower than the number of PNe and the future investigations will hopefully resolve this issue. At the moment, from the best-fitting values obtained using Newtonian approach, we can reach a strong conclusion that we can fit the kinematic data (for both families of tracers) with constant mass-to-light ratio models. However, the values obtained are higher than those based on the

SPS models, which implies that the additional, dark, component is required; the constraint that emerges from our analysis is that the dark matter density profile should not be significantly different from the stellar distribution over the range of scales the kinematic tracers are sensitive to. In any case, our findings suggest the lack of significant amount of dark matter in NGC 821.

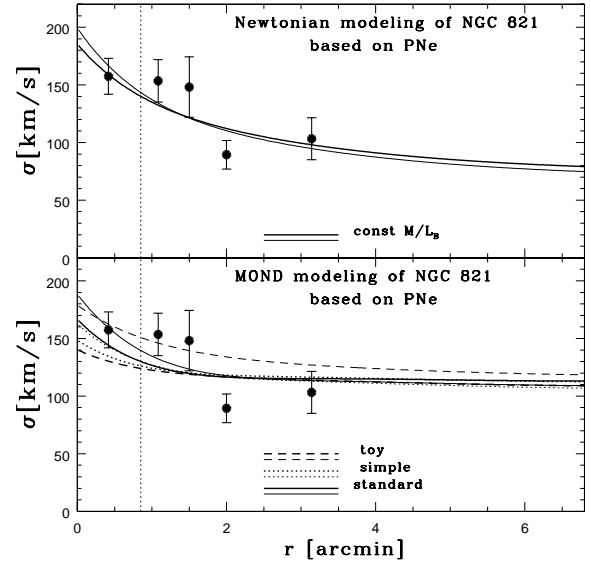


Fig. 3. The Jeans Newtonian and MOND modelling of the projected velocity dispersion of NGC 821 based on PNe; the thick lines are for isotropic cases and thin lines are for fits based on β_{th} . Upper panel: in the Newtonian approach, the mass-follows-light models are $M/L_B = 5.0$ (the thick solid line) and $M/L_B = 6.0$ (the thin solid line). Lower panel: the MOND models of the projected velocity dispersion of NGC 821 for three interpolation functions $\mu(r)$. The standard MOND model is presented with the thick (thin) solid line for $M/L_B = 4.0$ (5.4); the simple MOND model is presented with the thick (thin) dotted line for $M/L_B = 3.0$ (3.8); and the toy MOND model is presented with the thick (thin) dashed line for $M/L_B = 2.2$ (4.2). In both panels one effective radius is indicated by a vertical dotted line.

4.2. MOND models of NGC 821

In the lower panels of Figs. 3 and 4 the results of the Jeans models based on three MOND formulas are plotted: one can see that all of them can fit the observed velocity dispersion without the need of dark matter and that the standard MOND model requires the highest mass-to-light ratio. The best-fitting values are as follows:

²For the conversion from the r -band to the B -band, we used the absolute r magnitude of NGC 821 from Cappellari et al. (2013).

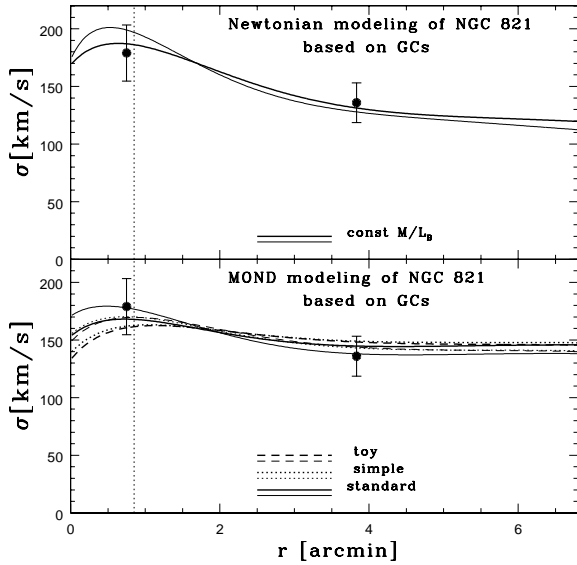


Fig. 4. *The Jeans Newtonian and MOND modelling of the projected velocity dispersion of NGC 821 based on GCs; the thick lines are for isotropic cases and thin lines are for fits based on β_{th} . Upper panel: in the Newtonian approach, the mass-follows-light models are $M/L_B = 9.4$ (the thick solid line) and $M/L_B = 11.8$ (the thin solid line). Lower panel: the MOND models of the projected velocity dispersion of NGC 821 for three interpolation functions $\mu(r)$. The standard MOND model is presented with the thick (thin) solid line for $M/L_B = 7.4(9.6)$; the simple MOND model is presented with the thick (thin) dotted line for $M/L_B = 5.8(7.6)$; and the toy MOND model is presented with the thick (thin) dashed line for $M/L_B = 4.4(5.9)$. In both panels one effective radius is indicated by a vertical dotted line.*

For the standard MOND model,
for PNe: $M/L_B = 4.0 \pm 1.0$ (isotropic case) and $M/L_B = 5.4 \pm 1.0$ (anisotropic case);
for GCs: $M/L_B = 7.4 \pm 1.8$ (isotropic case) and $M/L_B = 9.6 \pm 1.8$ (anisotropic case).

For the simple MOND model,
for PNe: $M/L_B = 3.0 \pm 0.6$ (isotropic case) and $M/L_B = 3.8 \pm 0.8$ (anisotropic case);
for GCs: $M/L_B = 5.8 \pm 1.4$ (isotropic case) and $M/L_B = 7.6 \pm 1.8$ (anisotropic case).

For the toy MOND model,
for PNe: $M/L_B = 2.2 \pm 0.6$ (isotropic case) and $M/L_B = 4.2 \pm 0.6$ (anisotropic case);
for GCs: $M/L_B = 4.4 \pm 1.0$ (isotropic case) and $M/L_B = 5.9 \pm 1.3$ (anisotropic case).

Again, the stellar mass-to-light ratios inferred from the MOND approach are in agreement with the SPS models although they are lower, and especially toy models predict much lower values.

The best-fitting values are plotted in Figs. 3 and 4 in the lower panel with thick (thin) solid lines for isotropic (radially anisotropic) cases for each of the three MOND models as indicated in the figures. From Fig. 3 one can notice that for PNe only the standard MOND model for both cases and simple MOND model for the radially anisotropic case can provide a fit for both inner and outer regions of NGC 821; the isotropic simple and toy MOND models can provide a fit of the outermost point and the radially anisotropic toy MOND model can provide a fit to the inner part (interior to $\sim 2R_e$) albeit with a higher value of the mass-to-light ratio than in the isotropic case ($M/L_B = 4.2$); no such problems exist in the case of the MOND models based on GCs.

Table 1. Kinematics of NGC 821 based on PNe

r	σ	err(σ)	s_3	err(s_3)	s_4	err(s_4)	N
arcsec	km s ⁻¹	km s ⁻¹					
(1)	(2)	(3)	(4)	(5)	(6)	(7)	(8)
25	157	16	-0.276	0.343	-0.616	0.686	51
65	154	18	-0.112	0.414	-0.059	0.828	35
90	148	26	-0.424	0.612	-0.438	1.224	16
120	89	12	-0.019	0.480	-0.356	0.961	26
189	103	18	-0.198	0.612	-1.210	1.224	16

NOTES – Col. (1): radius at which a given quantity is calculated. Col. (2): velocity dispersion. Col. (3): error of the velocity dispersion. Col. (4): s_3 parameter. Col. (5): error of the s_3 parameter. Col. (6): s_4 parameter. Col. (7): error of the s_4 parameter. Col. (8): number of given objects per bin.

Table 2. Kinematics of NGC 821 based on GCs

r	σ	err(σ)	s_3	err(s_3)	s_4	err(s_4)	N
arcsec	km s ⁻¹	km s ⁻¹					
(1)	(2)	(3)	(4)	(5)	(6)	(7)	(8)
45	179	24	0.149	0.471	-1.062	0.942	27
230	136	17	-0.954	0.440	2.106	0.880	31

NOTES – same as in the previous table.

5. CONCLUSIONS

In this paper we used two different populations of tracers belonging to the nearby early-type galaxy NGC 821, PNe (taken from T10) and GCs (taken from P13), in order to extract the kinematics which is then used for the purpose of dynamical modelling through solving the Jeans equation. Our results are as follows:

(1) The velocity dispersion of NGC 821 shows a declining trend: from the central value of 157 (179) km s⁻¹ it drops to 103 (136) km s⁻¹ for PNe (GCs). The departures from the Gaussian are small except for the outer bin in the case of the sample based on GCs where we have a hint of radial anisotropies.

(2) We solve the Jeans equation in order to establish the existence of dark matter in NGC 821. We applied two approaches for both populations of tracers assuming spherical symmetry: the Newtonian mass-follows-light and the MOND approach. For both populations we assumed two cases: isotropic case and radially anisotropic case. The best-fitting estimates of the mass-to-light ratio are compared with the SPS models in order to establish the contribution of dark matter. We find that we can fit the kinematic data with a constant mass-to-light ratio. However, the required values of the mass-to-light ratio are difficult to accommodate with normal stellar populations, therefore implying the existence of dark matter background, but with the constraint that the dark matter density profile can not be significantly different from the stellar distribution over the range of scales the kinematics tracers are sensitive to. We confirm the previous findings of T10 and Deason et al. (2012) that there is a lack of dark matter in the early-type galaxy NGC 821: our conclusion is based on the sample of PNe, i.e., the tracers that they used, but also on the recently published sample of GCs found in P13.

(3) Using the Newtonian approach, we estimated the following mass-to-light ratio of NGC 821: $4.2 < M/L_B < 7.0$ (for PNe sample) and $7.8 < M/L_B < 12.4$ (for GCs sample). The given ranges take into account possible radial anisotropies found in NGC 821 and they strongly suggest lack of the significant amount of dark matter in NGC 821.

(4) Using the MOND approach, we tested three MOND formulas: standard, simple and toy. The values of the established mass-to-light ratios suggest a lack of dark matter and the MOND the-

ory alone is capable of describing the dynamics of NGC 821 without invoking the additional dark component for both populations of tracers, PNe and GCs.

Acknowledgements – This work was supported by the Ministry of Education, Science and Technological Development of the Republic of Serbia through the project no. 176021, "Visible and invisible matter in nearby galaxies: theory and observations". This research made use of the NASA/IPAC Extragalactic Database (NED), which is operated by the Jet Propulsion Laboratory, California Institute of Technology, under contract with the National Aeronautics and Space Administration. We acknowledge the usage of the HyperLeda database (<http://leda.univ-lyon1.fr>). The authors gratefully acknowledge the valuable comments of the referee, which helped to improve the quality of the manuscript.

REFERENCES

- Bekenstein, J.: 2004, *Phys. Rev. D*, **70**, 083509.
 Bell, E. F. and de Jong, R. S.: 2001, *Astrophys. J.*, **550**, 212.
 Binney, J. J. and Mamon, G.: 1982, *Mon. Not. R. Astron. Soc.*, **200**, 361.
 Binney, J. J. and Tremaine, S.: 2008, *Galactic Dynamics*, Second Edition, Princeton Univ. Press, Princeton.
 Cappellari, M., Scott, N., Alatalo, K. et al.: 2013, *Mon. Not. R. Astron. Soc.*, **432**, 1709.
 Deason, A. J., Belokurov, V., Evans, N. W. and McCarthy, I. G.: 2012, *Astrophys. J.*, **748**, 2.
 Famaey, B. and Binney, J.: 2005, *Mon. Not. R. Astron. Soc.*, **363**, 603.
 Famaey, B., Gentile, G., Bruneton, J.-P. and Zhao, H. S.: 2007, *Phys. Rev. D*, **75**, 063002.
 Gerhard, O.: 1993, *Mon. Not. R. Astron. Soc.*, **265**, 213.
 Hernquist L.: 1990, *Astrophys. J.*, **356**, 359.
 Kroupa, P.: 2001, *Mon. Not. R. Astron. Soc.*, **322**, 231.
 Mei, S., Blakeslee, J. P., Côté, P., et al.: 2007, *Astrophys. J.*, **655**, 144.
 Milgrom, M.: 1983, *Astrophys. J.*, **270**, 365.
 Pota, V., Forbes, D. A., Romanowsky, A. J. et al.: 2013, *Mon. Not. R. Astron. Soc.*, **428**, 389 (P13).
 Richtler, T., Schuberth, Y., Hilker, M., Dirsch, B., Bassino, L. and Romanowsky, A. J.: 2008, *Astron. Astrophys.*, **478**, L23.

- Samurović, S.: 2007, *Publ. Astron. Obs. Belgrade*, **81**, 1.
Samurović, S.: 2010, *Astron. Astrophys.*, **514**, A95.
Samurović, S.: 2012, *Astron. Astrophys.*, **541**, A138.
Samurović, S. and Ćirković M. M.: 2008, *Astron. Astrophys.*, **488**, 873.
Sanders, R. H. and McGaugh, S.: 2002, *Annu. Rev. Astron. Astrophys.*, **40**, 263.
Teodorescu, A. M., Méndez, R. H., Bernardi, F., Riffeser, A. and Kudritzki, R. P.: 2010, *Astrophys. J.*, **721**, 369 (T10).
Tiret, O., Combes, F., Angus, G. W., Famaey, B. and Zhao, H. S.: 2007, *Astron. Astrophys.*, **476**, L1.
Tonry, J. L., Dressler, A., Blakeslee, J. P. et al.: 2001, *Astrophys. J.*, **546**, 681.

МАЛА КОЛИЧИНА ТАМНЕ МАТЕРИЈЕ У БЛИСКОЈ ГАЛАКСИЈИ РАНОГ ТИПА NGC 821

S. Samurović, A. Vudragović, M. Jovanović and M. M. Ćirković

Astronomical Observatory, Volgina 7, 11160 Belgrade 74, Serbia

E-mail: srdjan@aob.rs

УДК 524.7–333

Оригинални научни рад

У раду се анализира кинематика и динамика блиске галаксије раног типа, NGC 821, која се заснива на планетарним маглинама и глобуларним јатима у њеном саставу. У раду се користе планетарне маглине и глобуларна јата како би се израчунали кинематички параметри који се онда користе за динамичко моделирање путем Џинсове једначине. Џинсова једначина се користи у Њутновском приступу подразумевајући кон-

стантан однос маса-сјај како би се показало да је допринос тамне материје у овој галаксији мали: процењени однос маса-сјај, $4.2 < M/L_B < 12.4$, који важи у целој галаксији имплицира одсуство значајнијих количина тамне материје. У раду су коришћена и три различита MOND приступа и пронађено је да кинематички подаци могу да се фитују без додатне, тамне, компоненте.